Conversion of the dominantly ideal MHD perturbations into a tearing mode after a sawtooth crash

Revised 11/6/2014 14:53:00

V. Igochine[1], A. Gude[1], S. Günter[1], K. Lackner[1], Q. Yu[1], L. Barrera Orte[1], A. Bogomolov[2], I. Classen[2], R. M. McDermott[1] , N. C. Luhmann, Jr.[3] and ASDEX Upgrade team

[1]*Max Planck Institute for Plasma Physics, Boltzmannstr. 2, 85748 Garching, Germany*
[2]*FOM-Institute DIFFER, Dutch Institute for Fundamental Energy Research, 3430 BE Nieuwegein, The Netherlands*
[3]*University of California at Davis, Davis, California, CA 95616 USA-Institute*

e-mail address: valentin.igochine@ipp.mpg.de

Forced magnetic reconnection is a topic of common interest in astrophysics, space science and magnetic fusion research. The tearing mode formation process after sawtooth crashes implies the existence of this type of magnetic reconnection and is investigated in great detail in the ASDEX Upgrade tokamak. The sawtooth crash provides a fast relaxation of the core plasma temperature and can trigger a tearing mode at a neighbouring resonant surface. It is demonstrated for the first time that the sawtooth crash leads to a dominantly ideal kink mode formation at the resonant surface immediately after the sawtooth crash. Local measurements show that this kink mode transforms into a tearing mode on a much longer timescale $\left(10^{-3}s-10^{-2}s\right)$ than the sawtooth crash itself $\left(10^{-4}s\right)$. The ideal kink mode formed after the sawtooth crash provides the driving force for magnetic reconnection and its amplitude is one of the critical parameters for the length of the transition phase from a ideal into a resistive mode. Nonlinear two fluid MHD simulations confirm these observations.

Keywords: magnetic reconnection, tearing mode, tokamak
PACS: 52.35.Vd, 52.55.Fa, 52.55.Tn

Magnetic reconnection is one of the fundamental processes in magnetized plasmas and central to the understanding of the conversion of magnetic into thermal and kinetic energy in astrophysics, space science and magnetic confinement research. Such plasmas are often nearly collisionless, and the reconnection rates are thus much shorter than predicted by resistive MHD theory. The main difference between astrophysical and magnetic confinement plasmas is the existence of a strong magnetic guide field in the latter case [1]. This paper deals with forced magnetic reconnection in magnetic fusion plasmas. In tokamak plasmas, large sawtooth crashes typically produce fast relaxations of the core plasma density and temperature and provide the drive for magnetic reconnection at the neighbouring resonant surfaces with safety factor $q=m/n$, where m and n are integer numbers and represent the poloidal and toroidal mode numbers, respectively. Magnetic reconnection rearranges the magnetic topology at the resonant surface. It can start either from noise perturbations if the gradient of the plasma current at the resonant surface provides the drive for a tearing mode [2], or it requires an external drive at the start. The second situation is more common for neoclassical tearing modes (NTMs), which require a seed island to grow. The drive for the tearing mode is usually provided by background MHD instabilities (sawteeth, ELMs, etc.) [3,4,5]. When the critical island width is reached, the pressure profile becomes flat within the island, and the neoclassical drive takes over. Small islands are not able to provide significant pressure flattening and might be driven by other mechanisms [6, 7]. In this paper, only the mechanism of the seed island formation by strong internal drive due to sawteeth is investigated in detail. This type of tearing mode formation is considered to be one of the most dangerous for future fusion reactors like ITER [8], because large sawteeth provide the strongest internal magnetic perturbations compared to other possible triggers and are able to trigger the mode already at very small normalized pressure values [3,4]. Previous observations from different tokamaks, for example from JET [9] or TCV [10], report large island widths directly after the crash based on analysis of magnetic and SXR measurements. Such measurements show large amplitudes of the mode directly after sawtooth crashes also in our experiments, but they do not allow us to distinguish between kink and tearing mode (island) - like structure of the perturbation at the future NTM resonant surface. It is shown in this paper that an ideal perturbation, with the same helicity as the tearing mode, is generated around this surface by the crash and produces this strong signal. The mode leads to substantial reconnection and formation of an island only on a longer time scale.

In this paper, a combination of all main MHD diagnostics installed in ASDEX Upgrade is used to investigate the triggering process. These include: (i) two independent electron cyclotron emission diagnostics (ECE-Imaging [11] and standard ECE), (ii) magnetic coils, and (iii) Soft X-ray cameras. The ECE-Imaging diagnostic measures the local electron temperature along 14 radial lines of sight around the q=2 resonant surface, where the (m=2, n=1) mode is triggered by sawtooth crashes. The measurements span across the resonant surface, in the radial direction with a spatial separation of about 1.3cm. Standard ECE provides local measurements along a single line of sight which crosses the q=1 and q=2 resonant surfaces. Both diagnostics give information about local temperature perturbations inside the plasma, which depend on the temperature gradient ($\delta T_e = -\xi \cdot \nabla \langle T_e \rangle$, where ξ is the displacement). In the case of flat T_e profiles, temperature fluctuations are not visible. Thus, it is difficult to determine the perturbation amplitude from ECE measurements during a phase with strong evolution of the background temperature profile, which is the case directly after a sawtooth crash. Contrary to the ECE diagnostic, magnetic coils located outside the plasma are able to detect mode perturbations also in this case and provide a good indicator of the mode amplitude. The measured magnetic signal, Fourier filtered at the mode frequency, represents the total mode amplitude.

Rotation of an MHD mode with respect to the ECE measurement positions is used here to distinguish between kink and island-type structures. The idea is shown schematically in figure 1a. The measurement points 1 and 2 move along the dashed line during mode rotation. In this case, a perturbation caused by an ideal mode produces sinusoidal temperature variations in all channels around the resonant surface, and all these perturbations are in phase. The situation is different for an island structure, where the temperature inside the island is either flat or has an additional maximum (hot island case). In this case, the ECE signal is either flat within the island region or has an additional maximum. This feature gives a direct indication of the island separatrix position and the character of the mode (kink or tearing). This method of island identification avoids any further assumptions and allows for a direct identification of kink-tearing conversion directly. The temporal evolution of experimental ECE signals is shown in figure 1b for discharge 27257. The island structure is clearly visible in all ECE-Imaging channels from 7 to 2 at the end of the time window (t=2.782s). The saturated island width is thus about 6.4 cm. Backward tracing in time allows us to identify the point in time at which this feature appears for the first time in each of the channels (indicated by the dashed lines). All ECE signals are in phase before t=2.777s, which is a clear signature of an ideal kink perturbation. It should be noted that the amplitude of this ideal (2,1) mode is large immediately after the sawtooth crash (t=2.775), as can be seen from magnetic measurements in the bottom time trace of figure 1b.

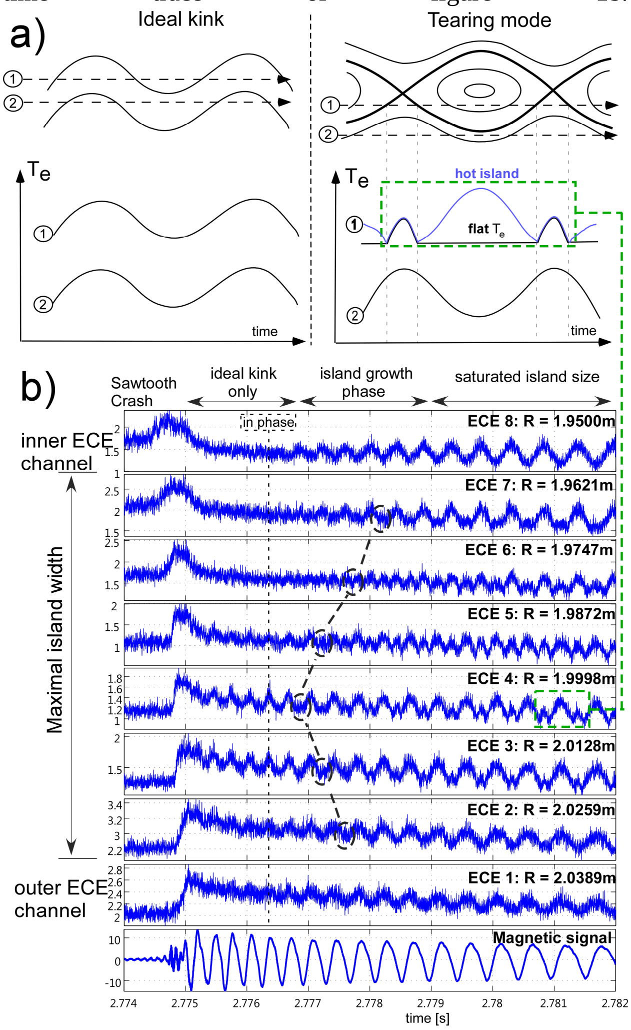

Figure 1. Identification of the island size from local ECE-Imaging measurements. a) Schematic representation of the temperature perturbation for the ideal kink case, island with flat temperature inside and hot island case. b) Direct identification of the transition from ideal kink mode into hot island in different ECE channels for discharge 27257 at t=2.77s. The bottom time trace is the magnetic signal $(d\tilde{B}/dt)$.

The same transition type is observed in the second case (#27257, t=2.5s), but the mode conversion time is much longer for this crash. The mode amplitude, $A_{(2,1)}$ is extracted from the magnetic measurements as $A_{(2,1)} \sim \sqrt{\hat{B}_{(2,1)}}$, where $\tilde{B}_{(2,1)}$ is the measured perturbation amplitude at the (2,1) frequency.

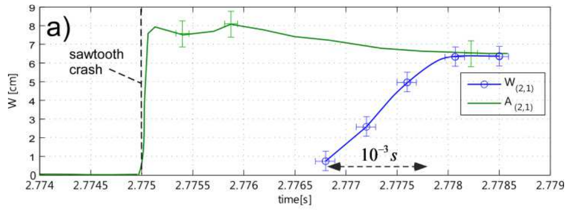

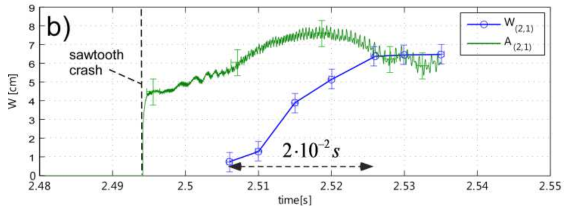

Figure 2. Comparison of the perturbation amplitude of the (2,1) mode from magnetic signals, $A_{(2,1)}$, and (2,1) island width , $W_{(2,1)}$, from ECE-Imaging measurements for two different cases: a) #27257, t=2.77s, the same case as in figure 1; b) #27257, t=2.5s. The mode amplitude from the magnetic signal is scaled to fit the island size from ECE at a later time point, when the saturated island size is reached. The error bars depend on the measurements resolution.

Figures 2a and b show the evolution of the magnetic mode amplitude in comparison with the island size from ECE. The sawtooth crash generates the ideal (2,1) mode directly after the crash. In figure 2a, the mode keeps its ideal character for about $2 \cdot 10^{-3}s$ and only then transforms into an island structure during $10^{-3}s$. In figure 2b the transition from ideal to tearing mode takes even longer. These time scales are much longer than the sawtooth crash time (about $10^{-4}s$ or less). It is interesting that the mode amplitude of the ideal mode directly after the crash differs almost by a factor of two in these two cases and is larger for the fast conversion case. The crash time itself, measured from fast ECE signals, is approximately the same in both cases. The magnetic signal remains the same during the mode conversion, which indicates that the kink mode and the resulting tearing mode have identical helicity (figure 1b, bottom, between 2.776s and 2.778s). The amplitude drops of the central ECE and SXR signals during the sawtooth crash in figure 2a are 32% and 40%, respectively, due to flattening of the temperature profile. For the second case (figure 2b), the drops are smaller (ECE 23%, SXR 24%) and the ideal mode amplitude immediately after the crash is smaller by almost a factor of two (figure 2).

There is a substantial difference to the case presented in Fig. 6a of ref. /10/ as evidence for generation of an island immediately after the sawtooth crash in TCV. There an island is inferred from SXR starting from the instant (800 μs after the crash) it is expected to become visible based on the amplitude of the magnetic signal and the relation assumed by the authors between its size and the measured perturbation field. No direct statement can be made on the existence of an island for the earlier phase, as it would be below detection threshold. In our case a period of 1.5 ms (2a) resp. 12 ms (2b) passes after the sawtooth crash during which no island can be detected although the magnetic perturbation would predict an island width of more than 5 cm which should have been clearly visible in ECE. Results reported on JET/9/ regarding the immediate appearance of a perturbation after the sawtooth crash actually refer only to magnetic signals and can therefore not contradict our findings.

The plasma rotation profiles are almost identical in these two cases, which excludes any influence of the rotation profile on the mode conversion time (figure 3). The same is true for kinetic profiles. The saturated island width, $W_{(2,1),sat} = 6.4[cm]$, is also the same for both cases, which is an indirect indication of similar plasma conditions.

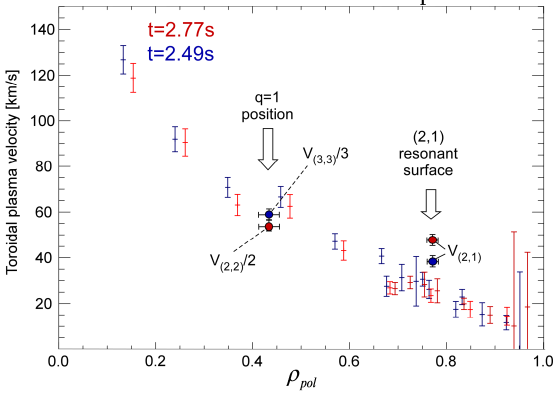

Figure 3. Toroidal plasma rotation for the same cases as in figures 1 and 2. Position of the q=1 and q=2 resonant surfaces are indicated as well as the (2,1) velocity after the crash and post-cursor velocity for (1,1).

Thus, the difference in the time scale of the mode conversion and in the delay of the tearing mode is probably connected to the different drives (different amplitudes of the ideal modes) after the sawtooth crash. The Sweet-Parker time required for the island formation is about *1s*. This time is much longer than the observed mode conversion times and shows the inapplicability of the single fluid reconnection picture as expected for collisionless fusion plasmas. This is also confirmed by comparison of characteristic lengths. Experimental plasma parameters at the (2,1) resonant surface show the ion-sound Larmor radius, $\rho_s = c_s/\Omega_i = 8.2 \cdot 10^{-3} m$, exceeds the width of the Sweet-Parker layer, $\delta_{sp} = L/\sqrt{S} = 1.2 \cdot 10^{-5} m$. Nonlinear two-fluid modelling of the NTM formation is discussed below.

A very important question is the origin of the ideal mode at the q=2 resonant surface after the sawtooth crash and its lasting presence after the crash. Spectral analysis of standard ECE signals shows the presence of the (2,1) mode simultaneously inside the q=1 surface and at the q=2 resonant surface after the crash. The central ECE channels, SXR and magnetics also show either a (2,2) or a (3,3) sawtooth pre-cursor and post-cursors in the two cases. The detected (2,2) mode has a frequency, which is twice the frequency of the following (2,1) mode. The (3,3) post-cursor has a frequency of 16.5kHz, which gives 5.5kHz for the (1,1) mode frequency after the crash. The detected (2,1) mode immediately after the crash has 3.5-4kHz in this case. This is smaller than the (1,1) frequency but higher than the plasma rotation at the q=2 surface, indicating a coupling of the (2,1) mode to a mode with higher natural rotation velocity, like the (1,1). The frequencies are transformed into rotation velocity and shown together with the measured plasma rotation in figure 3. Thus, a possible explanation for the existence of ideal (2,1) kink modes is a strong resistive (1,1) post-cursor, which drives the toroidally coupled (2,1) mode and keeps its amplitude at a relatively large value for a sufficiently long time after the sawtooth crash. The presence of sawtooth post-cursors is typical for ASDEX Upgrade [12].

A cylindrical, two fluids, non-linear MHD code is used to simulate the mode triggering [13,14]. Simulations use the measured experimental plasma parameters ($T_i = T_e = 600 eV$ as the temperatures at the q=2 surface, $q_a = 4$ as safety factor at the plasma edge, $n_e = 3 \cdot 10^{19} m^{-3}$ as the electron density, $B_t = 2.5T$ as the toroidal magnetic field, a Lundquist number of $S = 3.6 \cdot 10^7$, and a bootstrap current fraction of 10%). The triggering process is simulated by an imposed variation of a helical flux with (2,1) helicity at the plasma surface. This formulation is different from the experimental situation where the perturbation source is at the q=1 surface, but excludes the need to model the sawtooth crash post-cursor, which is a challenging task by itself. The results provide qualitative description of the process without direct relation between sawtooth crash amplitude and perturbed flux at the boundary. Additionally, the code uses a cylindrical approximation, which cannot describe toroidal coupling between (1,1) and (2,1) perturbations. Both diamagnetic effects and sheared poloidal plasma rotation are included and are essential for the dynamics of mode locking and island growth. The perturbed (2,1) flux is set to increase exponentially up to a saturated value on a very short time scale $\left(t_{growth} = 5 \cdot 10^{-5} s\right)$, comparable to the sawtooth crash time. After this time, the amplitude of the external (2,1) perturbation is kept constant, emulating the permanence of the perturbation after the crash in the experiment. Results of simulations with different amplitudes of the external perturbation in figure 4 show strong differences in the time-development of $A_{(2,1)}$, which in the case of tearing-type perturbations corresponds to the island width.

There is a transition value of the external flux amplitude, $\psi_{(2,1)} = 10^{-4}$, which corresponds to the slowly growing mode case in figure 2b. The amplitude of the perturbation below this value is not sufficient to slow down the plasma, and the perturbation remains essentially an ideal on Variation of the perturbation amplitude by a factor of two around this value leads either to transition to faster growth ($\psi_{(2,1)} = 2 \cdot 10^{-4}$) or to the absence of island growth ($\psi_{(2,1)} = 5 \cdot 10^{-5}$). Further increase of the perturbed amplitude gives only a moderate increase in the island growth. This bifurcation separates screening and penetration of the magnetic perturbation, with the latter case associated with slowing down of plasma rotation. Island growth also requires the persistence of the external drive, simulating a post-cursor perturbation in the sawtooth case. If the external helical drive is switched off after *100μs*, the mode decays and the perturbations are not sufficient to initiate the tearing mode growth, as shown for example in figure 4 for the $\psi_{(2,1)} = 2 \cdot 10^{-4}$ case. Similar results were also found for larger amplitudes. One should note here that two-fluid simulations with the same code have recently demonstrated that fast reconnection can be achieved within the two-fluid model applied. In fact, sawtooth simulations for realistic ASDEX Upgrade plasma parameters have resulted in reconnection rates like observed in experiments (<100μs) [15].

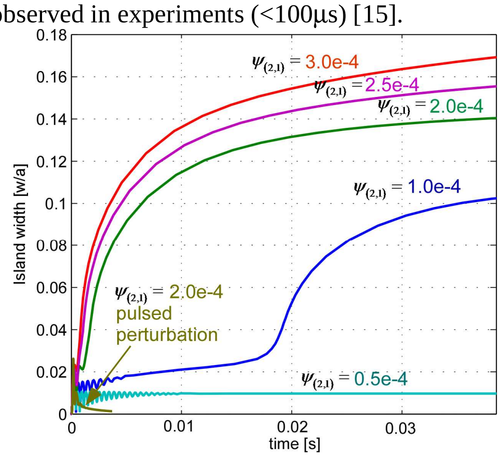

Figure 4. (2,1) perturbation field at the q=2 surface expressed in terms of an equivalent island width from two fluid non-linear MHD simulations. The evolution is given for different amplitudes of the perturbed flux at

the plasma boundary $\psi_{(2,1)} = 5\cdot10^{-5};10^{-4};2\cdot10^{-4};2.5\cdot10^{-4};3\cdot10^{-4}$.

The special case with pulsed perturbation is shown for $\psi_{(2,1)} = 2\cdot10^{-4}$.

The island evolutions in figures 2 and 4 are similar to the single fluid resistive MHD picture [16, 17, 18]: (i) ideal MHD phase, without island growth; (ii) Sweet-Parker phase, with fast island growth; (iii) Rutherford phase, with slow non-linear growth. At the same time, the physical mechanism in our case is completely different: (i) slowdown of the plasma rotation; (ii) optimal rotation for best flux penetration accompanied by fast island growth; (iii) non-linear evolution. The important result of our calculations and experiments is that the conversion time (for the plasma conditions studied) is always longer compared to the typical sawtooth crash time. A large tearing mode requires time for its formation and never appears directly after the crash. Thus, the existence of a driving force with sufficient duration is required for island formation. The transition time depends on the amplitude of this driving force. This dependence is strongly nonlinear.

Acknowledgement

This work was partially funded by the Max-Planck/Princeton Center for Plasma Physics.

[1] M.Yamada, R.Kulsrud, H.Ji, Rev.Mod.Phys. (2010) 603
[2] H.P.Furth, J.Killeen, M.N.Rosenbluth, Phys. Fluids, (1973),1054
[3]A.Gude, S.Günter, S.Sesnic, Nuclear Fusion, Vol.39 (19 99), p. 127
[4] S. Fietz, M.Maraschek, H.Zohm, M.Reich, L.Barrera, R .M.McDermott and the ASDEX Upgrade Team, Pl. Phys. Contr. Fus. 55 (2013) 085010
[5] F.M.deBock, I.G.J.Classen, C.Busch, R.J.E.Jaspers, H.R .Koslowski, B.Unterberg and the TEXTOR Teamet.al., Nucl. Fus.**48** (2008) 015007
[6] O. Sauter, C. Angioni, Z.R. Lin-Liu, Phys. Plasmas 6 (1999) 2834
[7] O. Sauter, R.J. Buttery, R. Felton, T.C. Hender, D.F. Ho well and contributors to EFDA-JET Workprogramme, Pl. Phys. Contr. Fus. 44 (2002) 1999
[8] T.C.Hender, J.C Wesley, J. Bialek, A. Bondeson, A.H. Boozer, R.J. Buttery, A. Garofalo, T.P Goodman, R.S. Granetz, Y. Gribov, O. Gruber, et.al., Nucl.Fusion 47 (2007) S128
[9] O. Sauter, E. Westerhof, M. L. Mayoral, B. Alper, P. A. Belo, R. J. Buttery, A. Gondhalekar, T. Hellsten, T. C. Hender, D. F. Howell, T. Johnson, P. Lamalle, M. J. Mantsinen, F. Milani, M. F. F. Nave, F. Nguyen, A. L. Pecquet, S. D. Pinches, S. Podda, and J. Rapp, Phys. Rev. Lett. 88 (2002) 105001
[10] G.P.Canal, B.P. Duval, F. Felici, T.P. Goodman, J.P. Graves, A. Pochelon, H. Reimerders, O. Sauter, D.Testa and the TCV Team, Nucl. Fusion 53 (2013) 113026
[11] I.G.J.Classen, J.E.Boom, W. Suttrop, E.Schmid, B.Tobias, C.W.Domier, N.C.Luhmann Jr., A.J.H. Donne, R.J.E. Jaspers, P.C. deVries, H.K.Park, T.Munsat, M. Garcia-Munoz and P. A. Schneider, Rev.Sci.Instr.81 (2010) 10D929
[12] V.Igochine, J. Boom, I. Classen, O. Dumbrajs, , S. Günter, K. Lackner, G. Pereverzev, H. Zohm and ASDEX Uprade Team, Phys. Plasmas 17, 122506 (2010)
[13] Q. Yu, S. Günter, K. Lackner and M. Maraschek, Nucl. Fusion 52 (2012) 063020
[14] Q. Yu, Nucl. Fusion 50 (2010) 025014
[15] S. Günter, K. Lackner, Q. Yu, *Fast sawtooth reconnection at realistic Lundquist numbers*, submitted to PPCF (2014)
[16] T. S. Hahmand R. M. Kulsrud, Physics of Fluids, 28, (1985) 2412
[17] X. Wang and A. Bhattacharjee, Physics of Fluids B, 4, (1992) 1795
[18] R. Fitzpatrick, Physics of Plasmas, 10, (2003) 2304